

## New Proposal for Sugarcane Vinasse Treatment by Hydrothermal Carbonization: An Evaluation of Solid and Liquid Products

Laís G. Fregolente,<sup>a</sup> Antonio J. R. de Castro,<sup>b</sup> Altair B. Moreira,<sup>a</sup> Odair P. Ferreira<sup>b</sup> and Márcia C. Bisinoti<sup>✉,a</sup>

<sup>a</sup>Laboratório de Estudos em Ciências Ambientais, Departamento de Química e Ciências Ambientais, Instituto de Biociências, Letras e Ciências Exatas, Universidade Estadual Paulista (Unesp), Campus São José do Rio Preto, Rua Cristóvão Colombo, 2265, 15054-000 São José do Rio Preto-SP, Brazil

<sup>b</sup>Laboratório de Materiais Funcionais Avançados (LaMFA), Departamento de Física, Universidade Federal do Ceará, CP 6030, 60455-900 Fortaleza-CE, Brazil

Vinasse is a residue of ethanol production from sugarcane. In view of the problems associated with its disposal, this study aimed to propose a treatment for vinasse by hydrothermal carbonization. The influence of temperature (100 to 200 °C), acidity (1.7 to 8.3%) and reaction time (12 to 48 h) on the hydrothermal treatment was evaluated, as well the characteristics of the solid (hydrochar) and liquid (process water) products. For the solid product, two hydrothermal carbonization conditions stood out as leading to higher carbonization and yields. These conditions were 200 °C, 8.3% acidity and times of 12 and 48 h. For the process water, the carbonization reaction at 200 °C, 8.3% acidity and 48 h produced the highest discoloration and 77% reduction of total organic carbon. Thus, hydrothermal carbonization proved to be an efficient method to treat vinasse, and the hydrochar presents potential for use as fertilizers / soil conditioners, and also the process water after pre-treatment.

**Keywords:** hydrothermal carbonization, sugarcane, hydrochar, process water, reuse

### Introduction

Brazil is the world's largest producer of ethanol from sugarcane. In this process the broth is fermented and then distilled, generating ethanol as product and vinasse as liquid residue. For each liter of alcohol produced, 10 to 18 L of vinasse are generated,<sup>1,2</sup> which has high concentrations of organic matter (13.38-32.6 g L<sup>-1</sup> as chemical oxygen demand (COD)), potassium (1200-2056 mg L<sup>-1</sup>), calcium (719-840 mg L<sup>-1</sup>), sodium (50.2-114 mg L<sup>-1</sup>) and magnesium (237-320 mg L<sup>-1</sup>).<sup>1-4</sup> Vinasse is used mainly in soil fertigation.<sup>1</sup> This practice can cause problems for agriculture and livestock; the application of vinasse to the soil in large quantities can generate the formation of vinasse puddles, which present ideal conditions for the development, for example, of the stable fly, as well as causing discomfort due to its bad smell. The stable fly feeds on bovine blood, promoting stress conditions to the cows, reducing milk production or making weight

gain difficult.<sup>5</sup> Fertigation can also lead to problems such as soil salinization,<sup>6</sup> groundwater contamination<sup>7,8</sup> and it may cause damage to aquatic life, depending on the concentration, due to its toxic effect causing morphological changes and fish death.<sup>4</sup>

Both the technological and scientific literature present several proposals for treatment or use of vinasse. For example, the patents PI 1100736-2<sup>9</sup> and WO 2014/098874<sup>10</sup> propose a system for treatment of vinasse in an anaerobic reactor with generation and collection of biogas. In the second one, it is suggested that the process generates a salt solution which contains mineral nutrients that can be used as fertilizer. Carbonation processing of vinasse for carbon fixation and turbidity reduction for its use as a culture medium for the cultivation of microorganisms was proposed in PI 1106809-4.<sup>11</sup> A process to recycle vinasse and carbon dioxide arising from burning of bagasse in alcohol distilleries and the sugar industry through algal cultivation and processing was proposed in PI 0706144-7,<sup>12</sup> and equipment for the production of organic-mineral fertilizer by electric discharge with

\*e-mail: mbisinoti@hotmail.com

sufficient energy to degrade the organic material was proposed in PI 0401563-0.<sup>13</sup> El-Dib *et al.*<sup>14</sup> proposed the removal of color and the reduction of organic carbon in vinasse by adsorption on modified bentonite and chitosan. Seixas *et al.*<sup>15</sup> reported the adsorption of vinasse organic carbon by activated carbon obtained from sugarcane bagasse. Physicochemical treatments of organic matter with Fe<sup>2+</sup>-activated persulfate and peroxy monosulfate oxidation, and treatments in anaerobic digesters and ponds, have also been studied.<sup>16-18</sup> However, the processes developed so far have not been able to solve the problem totally; research and development into new ways to treat these effluents are still necessary.

Hydrothermal carbonization (HTC) has been applied to prepare carbon-rich materials, starting from different feedstocks, such as sugars, polysaccharides, biomass and biomass residues, wastewater and slurry.<sup>19-22</sup> This process takes place in aqueous medium and at intermediate temperatures (150-350 °C), and the pressure in the reactor is self-generated by water vapor. Thus, the process pressure is dependent on the temperature and the reactor filling volume.<sup>23-25</sup> Among the many advantages of HTC, the possibility of using humid biomass was the one that led us to consider the treatment of vinasse from the sugarcane industry using this methodology,<sup>26-28</sup> making it possible to produce a carbonaceous material rich in nutrient. Some authors<sup>29-31</sup> have investigated the viability of HTC, showing that the amount of energy required by the process will depend especially on the hydrothermal process parameters, as reaction time, dry biomass / water ratio and temperature.

Recently, our research group reported the HTC of vinasse and sugarcane bagasse mixture in the presence of phosphoric acid, generating hydrochar with N, P, K and Ca,<sup>32</sup> and also in the presence of base and salts aiming at greater immobilization of nutrients in hydrochar,<sup>33</sup> both presenting potential for use in agriculture. The characteristics of the products generated in HTC will depend on the feedstock and also on the process conditions, such as temperature, reaction time and reaction medium pH.<sup>26</sup> This allows a wide use of the solid product generated, which can be used as a source of energy, as a solid fuel<sup>34,35</sup> or as soil conditioner.<sup>26,36,37</sup> Therefore, a new proposal of vinasse treatment using HTC was explored in this work, varying the reaction parameters such as reaction time, temperature and percentage (v/v) of H<sub>2</sub>SO<sub>4</sub> in the reaction medium, evaluating not only the carbonization and the immobilization of nutrients in hydrochar but also the reduction of turbidity, total organic carbon (TOC) and mineral content in the process water.

## Experimental

### Treatment of vinasse using HTC

HTC reactions of the vinasse were carried out in a 90 mL stainless steel reactor, coated with temperature-resistant polymeric material. Ten reactions were conducted, varying the reaction time, H<sub>2</sub>SO<sub>4</sub> percentage (v/v) and temperature (Table 1). The reactions were divided into three groups according to the carbonization temperatures. Thus, the 4 reactions performed at 100 °C belong to group C (named C1, C2, C3 and C4), the 5 reactions performed at 200 °C belong to group D (named D0, D1, D2, D3 and D4), and group M has just one reaction processed at 150 °C named M.

**Table 1.** Reaction parameters used in HTC processes

Reaction	Temperature / °C	Acidity / % (v/v)	Residence time / h
C1	100	1.7	12
C2	100	8.3	12
C3	100	1.7	48
C4	100	8.3	48
M	150	5.2	30
D0	200	0.0	48
D1	200	1.7	12
D2	200	8.3	12
D3	200	1.7	48
D4	200	8.3	48

C1-C4: reactions performed at 100 °C; M: reaction performed at 150 °C; D0-D4: reactions performed at 200 °C.

In these experiments 55.0 mL of vinasse (mass of approximately 57.0 g) and varying amounts of sulfuric acid making up 1.7, 5.2 or 8.3% v/v were added to the reactor. Subsequently, for the hydrothermal treatments, the reactor was closed and heated in a muffle furnace to 100, 150 or 200 ± 10 °C for 12, 30 or 48 h (Table 1) according to each reaction as shown in Table 1, following as it is described in patent PI 102015003018-5.<sup>38</sup> A reaction was also conducted at 200 °C in the absence of sulfuric acid. After the hydrothermal treatments, the reactor was cooled to room temperature and the suspension was vacuum filtered using a 0.45 µm acetate / cellulose membrane. The liquid phase (process water) was stored and the hydrochar was washed with deionized water to pH 4-5, and then dried until constant mass.

### Hydrochar characterization

#### Recovered mass

Calculation of mass recovered (hydrochar) was made by equation 1:

$$\text{Yield (\%)} = \frac{\text{Mass recovered}}{(\text{Feedstock mass} + \text{H}_2\text{SO}_4 \text{ mass})} \times 100 \quad (1)$$

where the feedstock mass is the mass of 55.0 mL of vinasse dried at 105 °C in an oven until constant weight (11.2353 g) and the H<sub>2</sub>SO<sub>4</sub> mass is the mass corresponding to 1.7, 5.2 or 8.3% of H<sub>2</sub>SO<sub>4</sub> added.

#### Fourier transform infrared spectroscopy (FTIR)

The spectra of the hydrochar in the infrared region were obtained using a Spectrum Two - UART Two (PerkinElmer) spectrometer, coupled to an attenuated total reflectance (ATR) accessory. The solid material was placed directly on the diamond crystal of the ATR accessory, and the spectra were obtained in the range 4000-400 cm<sup>-1</sup>, with resolution of 1 cm<sup>-1</sup> and 20 scans.

#### Elemental analysis (CHNS)

The determination of carbon, hydrogen, nitrogen and sulfur was made with an EA 1108 CHNS elemental analyzer (Fisons). The determinations of the ash in the hydrochars were made following the 2540G method,<sup>39</sup> and the oxygen concentrations were determined by equation 2:

$$\%O = 100 - (\%C + \%N + \%H + \%S + \%ash) \quad (2)$$

#### X-ray diffraction (XRD)

The XRDs of the solids (powder) were measured using CuK $\alpha$  radiation ( $\lambda = 1.5406 \text{ \AA}$ ) generated at 40 kV voltage and 40 mA current in a D8 Advance diffractometer (Bruker) with Bragg-Brentano geometry. The angular range of the measurements (in 2 $\theta$ ) was 5 to 65°, using steps of 0.02° and accumulation time of 1 s *per step*.

#### Scanning electron microscopy (SEM)

SEM images were obtained by an INSPECT 50 microscope (FEI Company). The samples were sprayed onto carbon tape, affixed on an aluminum stub, and coated with gold for the analyses by the sputtering technique using a Quorum Q150TES equipment. The images were obtained using a secondary electron (SE) detector and beam voltage between 5 and 20 kV.

#### Nutrients determination in hydrochar

First, the hydrochars were subjected to acidic decomposition for nutrient determination with nitric acid and hydrogen peroxide following the 3050B method,<sup>40</sup> The concentrations of Na, Al, Ca, K, Mg, Fe, Cu and Zn were determined by flame atomic absorption spectrometry (FAAS) using an AA240FS equipment (Varian), being Na and K determined in the emission mode. The dilutions of

the samples were made when necessary, depending on the concentration of the samples in relation to analytical curve. The instrumental conditions for FAAS analysis are in the Supplementary Information (SI) section (Table S3). The laboratory, where the samples were quantified, participates in the Embrapa Proficiency Assay for metal analysis in dry samples (plant tissue) and all results are considered to be very good ( $z \leq 2$ ).

#### Characterization of vinasse and process water

The vinasse and process water acidic decomposition were performed using nitric acid and hydrogen peroxide, following method 3010A<sup>41</sup> for the determination of nutrients. The concentrations of Na, Al, Ca, K, Mg, Fe, Cu and Zn were performed by FAAS using an AA240FS (Varian) being Na and K determined in the emission mode. The dilutions of the samples were made when necessary, depending on the concentration of the samples in relation to analytical curve. The instrumental conditions for FAAS analysis are in Table S3, SI section.

TOC was quantified by a TOC-VCSN analyzer (Shimadzu). The turbidity was determined using the HI 93703 multiparameter turbidimeter (Hanna Instruments). The color was determined by an HI 96727C portable photometer (Hanna Instruments). The pH determinations were performed using an MA PA200 pHmeter (Marconi), and conductivity was measured with an MA CA150 conductivity meter (Marconi).

## Results and Discussion

The vinasse used in these experiments presented 76.2 g L<sup>-1</sup> of TOC, pH of 4.2, conductivity of 44.1 mS cm<sup>-1</sup> and concentrations of 21.7 g L<sup>-1</sup> of K, 2.7 g L<sup>-1</sup> of Ca, 3.6 g L<sup>-1</sup> of Mg, 0.4 g L<sup>-1</sup> of Al, 0.2 g L<sup>-1</sup> of Fe, 0.3 g L<sup>-1</sup> of Na, 0.2 g L<sup>-1</sup> of Mn, 3.2 mg L<sup>-1</sup> of Cu and 6.0 mg L<sup>-1</sup> of Zn.

#### Hydrochars

##### Recovered mass

The HTC process of the vinasse generated a hydrochar (solid fraction), and a liquid fraction (termed “process water”). The gas fraction was not analyzed. The recovered mass of hydrochar (Table 2) was calculated according to equation 1.

Group C reactions resulted in 7-14% of recovered mass (Table 2). Thus, most of the precursors (organic matter and salts) remained dissolved or suspended in the process water. This fact corresponds with the high concentration of TOC (59-69 g L<sup>-1</sup>) and with the high conductivity found

**Table 2.** Masses of hydrochars obtained from hydrothermal processes, recovered masses, ash of the hydrochars and TOC concentrations and conductivity of the process waters

Reaction	Hydrochar			Process water	
	Hydrochar mass / g	Recovered mass / %	Ash / %	TOC / (g L <sup>-1</sup> )	Conductivity / (mS cm <sup>-1</sup> )
Vinasse	–	–	19.4	76.2	44.1
C1	1.49	11.4	11.3	68.9	70.7
C2	1.46	7.2	21.9	63.4	370.0
C3	1.78	13.6	6.0	58.9	63.7
C4	1.61	7.9	21.5	63.1	314.2
M	1.96	11.8	14.5	63.0	200.9
D0	2.04	18.2	17.5	45.0	47.1
D1	2.18	16.7	4.7	42.7	71.0
D2	4.09	20.2	10.5	17.1	250.4
D3	2.16	16.6	13.8	43.8	78.9
D4	4.31	21.3	9.0	17.3	157.1

TOC: total organic carbon; C1-C4: reactions performed at 100 °C; M: reaction performed at 150 °C; D0-D4: reactions performed at 200 °C.

in the process waters. In the M reaction, the recovered mass was 12%. The concentration of TOC in the process water was also high (63.0 g L<sup>-1</sup>), with values close to those found for group C reactions. The recovered masses for group D reactions were 17-21%, and higher recovered mass occurred in reactions with higher percentages of acid. Consequently, these reactions with higher recovered mass (D2 and D4) showed lower TOC concentrations in the process water (17.1 and 17.3 g L<sup>-1</sup>).

These results indicate that increase in reaction temperature promoted an increase in recovered mass of hydrochar (Table 2). The HTC process of the biomass was intensified at higher temperatures, converting the dispersed / soluble biomass of the vinasse into hydrochar.<sup>42</sup> Consequently, lower process water TOC concentration was observed as the recovered mass of hydrochar increased. The effect of the parameters applied to hydrothermal process (temperature, residence time, and acidity) with respect to the amount of recovered mass of hydrochar was evaluated by a Pareto chart, and the dependence and importance of temperature in the hydrothermal reactions was confirmed (see Figure S1, SI section). The Pareto chart showed that temperature was the most important factor to hydrochar mass. The combination of the temperature and acidity was the second factor that most influenced in the recovered mass. Additionally, this analysis suggests that the other factors evaluated, together or separated, did not affect the amount of recovered mass.

As shown by Pareto chart, the time intervals used in the reactions in this work did not significantly influence recovered mass. This was also noted by evaluating the recovered mass of the reactions performed under the same

conditions of temperature and acid percentage but with different reaction times (e.g., D1 and D3, or for C2 and C4). The recovered mass and concentrations of TOC found were similar, between D1 and D3, and also between C2 and C4, indicating that temperature and medium acidity parameters are the factors that directly influence both hydrochar yield and the process water TOC concentration obtained from vinasse carbonization.

#### Physical and chemical properties

The HTC process was evaluated using the Van Krevelen diagram (Figure 1). The elemental composition of the hydrochars varied according to the reaction conditions. O / C and H / C atomic ratios were observed to decrease with increasing temperature. These results are in agreement with those reported by Parshetti *et al.*<sup>43</sup> and Sevilla and Fuertes.<sup>44</sup> Note that the hydrochars can be separated into distinct groups, as shown in Figure 1, as the lower the H / C and O / C atomic ratios, the higher the degree of carbonization of the hydrochar. In the carbonization process, the reduction of hydrogen and oxygen content occurs due to the reactions that lead to the dehydration of the biomass. Other processes can also occur, such as decarboxylation<sup>45</sup> and demethanation<sup>46</sup> reactions, resulting in a more carbon-rich material, consequently reducing the H / C and O / C ratios compared to the starting biomass. Thus, the hydrochars with the highest degree of carbonization were those obtained in reactions D2 and D4 (group 3, Figure 1). Higher H / C and O / C ratios are observed for group C, indicating material with a lower degree of carbonization (group 1, Figure 1). It is worth mentioning that the hydrochar produced in



the D0 reaction (see Table 1) is also within group 1, in which no sulfuric acid was added. Therefore, the addition of acid is fundamental for the process of carbonization of the vinasse, since even the hydrochar produced by the D0 reaction, conducted at 200 °C without acid, showed a composition similar to those obtained at 100 °C, but in the presence of acid.

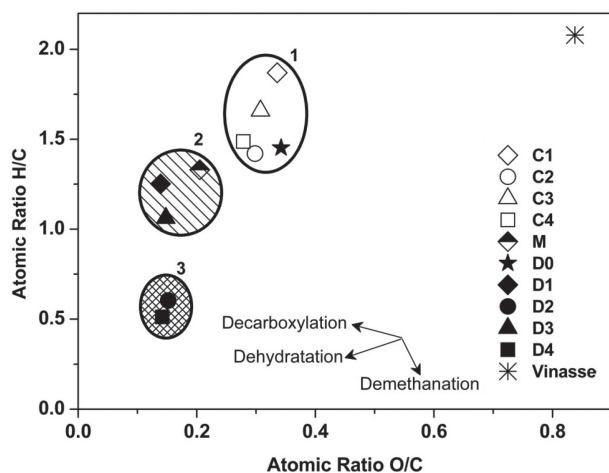


**Figure 1.** Van Krevelen diagram for the hydrochar samples obtained by HTC of vinasse and for the dried vinasse.

The low H / C atomic ratio indicates the presence of aromatic domains in the hydrochar structure. The composition of the material can be linked directly to its recalcitrance, i.e., its resistance to microbiological decomposition. So, the stability of the carbonaceous material is associated with its composition. Spokas<sup>47</sup> suggested that biochars with an O / C ratio of 0.6 would be stable, with an estimated half-life of more than 100 years, and carbonaceous materials with O / C atomic ratios lower than 0.2 would have stabilities of over 1000 years. Therefore, biochars with such characteristics when applied to soil are sources of carbon sequestration due to their recalcitrance.<sup>48</sup> In this context, the low O / C ratio of the hydrochars produced in this work, 0.14 (for D4) and 0.34 (for C1), suggest that if applied to the soil, they could also act in a similar way.

Figure 2 shows the FTIR spectra of vinasse and hydrochars. The position ( $\text{cm}^{-1}$ ), and relative intensities, and the absence of some bands attributed to biomass, or the presence of new bands in the hydrochars FTIR spectra, were used to evaluate the transformation that the vinasse underwent in the hydrothermal treatment process under different reaction conditions. Thus, significant changes in the vinasse spectral profile were observed compared to those of the final products (Figures 2a and 2b). In general, the wide bands at  $3500\text{--}3000\text{ cm}^{-1}$  of the hydrochars can be attributed to the O–H stretches of adsorbed water

molecules, alcohols and carboxylic acids present in the carbon chains of the hydrochars. Symmetrical and asymmetric stretch vibrations of aliphatic  $\text{CH}_2$  and  $\text{CH}_3$  can be observed in the  $2990$  and  $2800\text{ cm}^{-1}$  region, respectively. At approximately  $1707\text{ cm}^{-1}$ , bands were observed which can be attributed to the C=O carbonyl stretch of carboxylic acids, ketones, quinones and esters. Also, at  $1610\text{ cm}^{-1}$ , bands related to C=C vibrations of aromatic rings were observed for all hydrochars spectra, except for D2 and D4, where these were observed in  $1580\text{ cm}^{-1}$ . In addition,  $1373\text{ cm}^{-1}$  bands attributed to the deformation of aliphatic  $\text{CH}_3$ , and at approximately  $1105\text{ cm}^{-1}$  for the C–O of alcohols and phenols and / or vibrations of the remaining glycosidic skeleton from cellulose suspended in the vinasse are reported, usually present in the region of  $1050$  to  $1200\text{ cm}^{-1}$ .<sup>49–51</sup> In this region, the spectra of samples D2 and D4 presented only one broad band at  $1170\text{ cm}^{-1}$ .

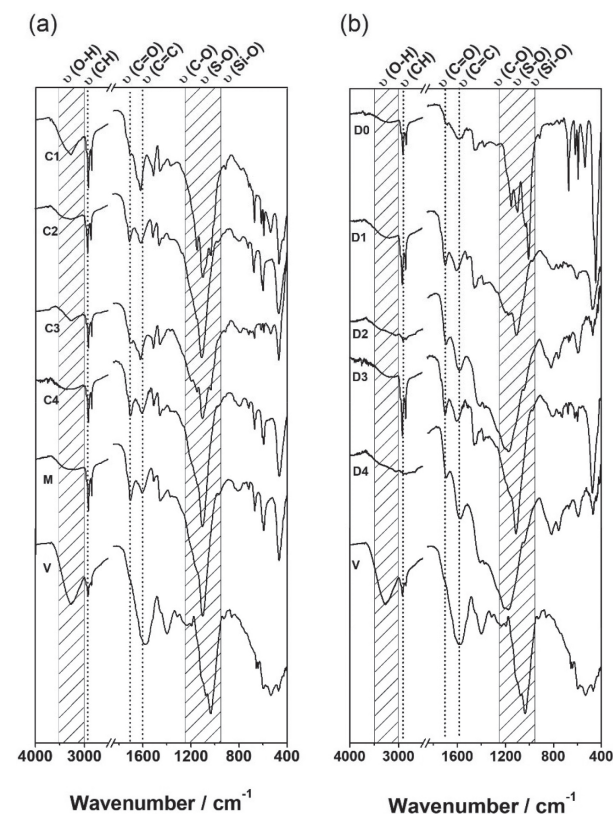


**Figure 2.** FTIR spectra of the hydrochars for (a) the groups C, M and vinasse (V) and for (b) group D and vinasse (V).

In addition to the bands related to the chemical groups characteristic of the carbon chains in hydrochars, the FTIR spectra could also give information regarding the inorganic phases present in the carbonaceous material. For example, the wide bands in the region of  $1250\text{--}950\text{ cm}^{-1}$  followed by the low intensity band at  $670\text{ cm}^{-1}$  may be the contribution of S–O vibrations of sulfate ions,<sup>52</sup> and related vibrations

of Si–O–Si in SiO<sub>2</sub>;<sup>53</sup> these attributions are in agreement with the XRD measurements.

For group C, the intensity decreases of the band at 3000–3500 cm<sup>-1</sup> in the hydrochars, when compared to that observed in the vinasse, occurred at the same time that the bands attributed to the C=O and C–O vibrations were intensified. In the meantime, the displacement of the maximum of the intense band occurs at higher wavenumbers, in the region of 1250–950 cm<sup>-1</sup>. The intensity reduction of the first band suggests that hydrolysis and dehydration occurred during the carbonization of the vinasse. On the other hand, the appearance of the band attributed to C=C stretch indicated the occurrence of polymerization and aromatization in the carbon chains of the hydrochars. If we compare the intensities of the bands attributed to C=O and C=C stretch between C1 and C2 and between C3 and C4 reactions, it can be observed that the increase in acid percentage in the reaction medium promoted an increase in the intensities of the C=O bands, which suggests a higher concentration of these functional groups in the carbonaceous material due to carbon oxidation. This indicates that the control of the reaction conditions can favor the specificity of functional groups present in the solid material. The change in the larger and more intense band to the higher wavenumber in the region of 1250–950 cm<sup>-1</sup> may mean the reduction of the intensity of the C–O vibrations and a greater contribution of inorganic phases in this region; as an example, those made up of sulfate ions.

The influence of sulfuric acid on vinasse carbonization reactions can be verified, once again, analyzing the FTIR spectra of the hydrochars of group D. For the sample D0, it is observed that the band attributed to C=O stretch presents low intensity when compared to that of the other hydrochars. The wide band around 1250–950 cm<sup>-1</sup> also presents a more distinct profile than the other samples, suggesting a lower degree of carbonization, corroborating the information described in the Van Krevelen diagram (Figure 1). Another point to highlight in the spectra of group D is that we can see clearly that the spectral profile of samples D2 and D4 are distinct from the others. An important confirmation is the almost total absence of the bands attributed to the C–H vibrations and displacement to smaller wavenumber of the bands attributed to the C=C stretch. These observations suggest a higher degree of carbonization of these samples, corroborating the results shown in the Van Krevelen diagram (Figure 1), which indicates that samples D2 and D4 (8.3% acid) probably also underwent demethanation reactions, as well as dehydration and aromatization, during the hydrothermal treatment. Thus, the highest concentrations of sulfuric acid, at 200 °C,

provide the breaking of aliphatic chains, evidenced by the disappearance of the bands in the region of 2990–2800 cm<sup>-1</sup>, referring to the vibrational modes of aliphatic CH<sub>2</sub> and CH<sub>3</sub>. There is also an increase in aromatization of hydrochar, evidenced by the displacement of the band attributed to C=C vibrations to 1580 cm<sup>-1</sup> in samples D2 and D4.<sup>44</sup> Also, the band attributed to the C=O vibrations of carboxylic acids for sample D4 and D2 presented lower intensity when compared to those of the other hydrochars.

Information of the hydrochar structure was accessed by XRD (Figure 3). In general, all the hydrochar diffractograms showed a low intensity peak between 10 and 35° (2θ), with a maximum at approximately 21–24° (2θ), indicating the presence of a material with low structural order (Figure 3b). Additionally, in the diffractograms, fine and intense peaks can also be observed, which overlap the wide peak, suggesting the existence of crystalline phases (Figure 3a).

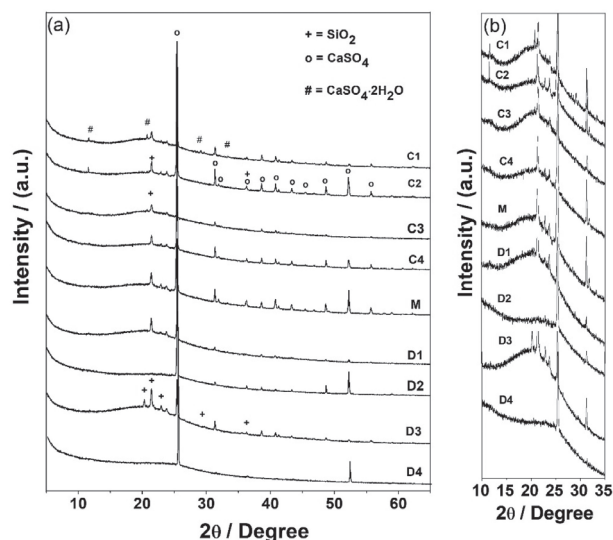


**Figure 3.** (a) XRD of the hydrochars obtained under different reaction conditions in the range of 5 to 65° (2θ) and (b) XRD for the range of 10 to 35° (2θ), showing the intensity of the wide peak approximately at 21–24° (2θ).

The low intensity wide peak centered at approximately 21° (2θ) for the samples of groups M and C could be attributed to the irregular orientations of the polycyclic aromatic chains which had not yet formed ordered domains, and which would provide reflections typical of graphite with a hexagonal unit cell (Inorganic Crystal Structure Database (ICSD) 076767). Therefore, the hydrochars obtained presented similar structural properties to amorphous carbon.<sup>54,55</sup> However, for samples D2 and D4, a shift of the maximum wide peak to higher angles was observed, with a maximum around 23–24° (2θ). This displacement is due to the higher degree of carbonization of these samples, which

represents a reduction of the interplanar distance, probably with the production of more graphitized domains but still with low structural order compared to crystalline graphite (ICSD 076767). This observation is consistent with the results described in the Van Krevelen diagram and the FTIR spectra (Figures 1 and 2, respectively).

The XRD also showed that along with the hydrochar crystalline phases related to  $\text{CaSO}_4 \cdot 2\text{H}_2\text{O}$  (ICSD 002057) (sample C1) and  $\text{CaSO}_4$  (ICSD 15876 or 01956) for the other samples of groups C and D are found. The presence of sulfates in hydrochars has also been suggested by the FTIR spectra. In addition to these inorganic phases, it was also possible to identify the presence of  $\text{SiO}_2$  in different crystalline systems (ICSD 15321, 34925 and 41672). This phase was also suggested by the FTIR spectra. Calcium sulfate would have its origin in the calcium precipitation reaction with the sulfate of the sulfuric acid used in the hydrothermal reactions, since Ca was present in vinasse at sufficiently high concentration. On the other hand, the existence of  $\text{SiO}_2$  would possibly have its origin in the vinasse itself. Furthermore, the presence of these inorganic phases in the hydrochar justifies the high ash content obtained for these materials (Table 2).

The morphology of the hydrochars was evaluated by SEM (Figure 4). In general, these carbonaceous materials presented spherical and irregular morphology and particle sizes of the order of few micrometers. For reactions D3 and D4, a large number of spherical particles was observed, whereas for reaction C1 it was observed that the majority of particles presented a rather irregular morphology. Thus, as the temperature and percentage of acid in the reaction medium increased, an increase in the number of spherical particles of hydrochar was observed, as was also observed by Melo *et al.*<sup>32</sup> in the carbonization of vinasse and sugarcane bagasse in the presence of phosphoric acid. For samples D3 and D4, it was possible to compare the difference in the characteristics of the material caused only by the difference in the acidity of the medium, where a higher percentage of acid (D4, Figure 4) provided more well-defined spheres with smoother surfaces, whereas the lower percentage of acid (D3, Figure 4) resulted in the formation of relatively few spheres, with a regular surface. A similar behavior was reported for carbon spheres obtained from the hemicellulose of the trunk of *Cannabis sativa* L., which presented smoother surfaces when obtained in the presence of higher acid concentration.<sup>56</sup>

The literature has shown that spheres of the order of a few micrometers are obtained by HTC of carbohydrates such as cellulose, sucrose and glucose, among others.<sup>44,57</sup> Therefore, the presence of spheres in the hydrochars produced from the HTC of vinasse would be due to the

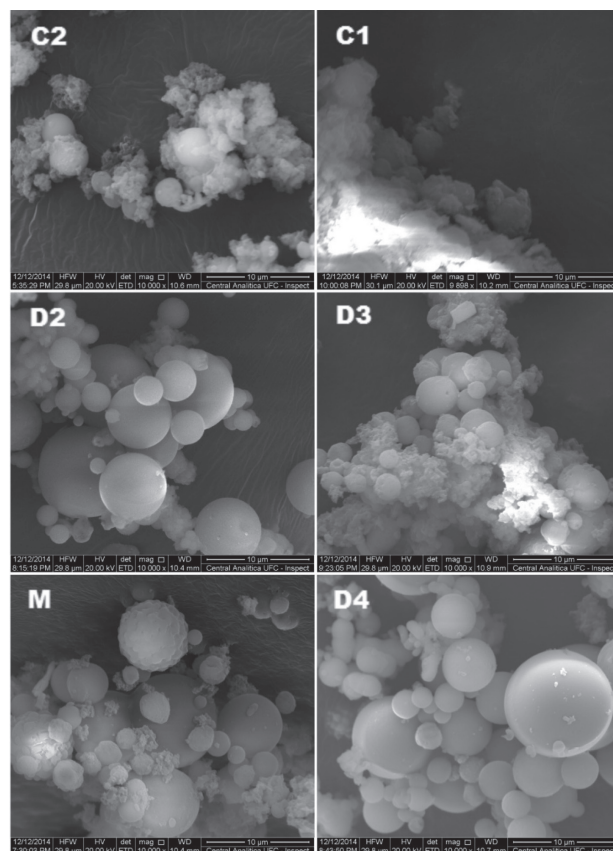


**Figure 4.** SEM images for samples of hydrochars C1, C2, M, D2, D3 and D4.

presence of unfermented sucrose residues and cellulose in suspension (cellulose coming from sugarcane stalks). Irregular morphologies could be associated with organic matter with a low degree of carbonization (SEM images of group C samples were difficult to obtain due to electrostatic loading), as well as deposition of carbon on the inorganic phases and / or it could be just the inorganic phases.

The results of the recovered nutrients in the hydrochars and process water from vinasse are shown in Figure 5. The figure shows the amount of each nutrient remaining in hydrochar and process water in relation to the total amount added to the reaction medium by the use of vinasse. The percentage of each nutrient should be inferred only by the relative percentage of the bar length represented by the color of the respective nutrient. For example, approximately 20% of the calcium initially present in the reaction medium remained in “C1 Hydrochar” (Figure 5a) and 5% remained in “C1 Process Water”. Note that the relative concentrations of potassium, sodium, iron and magnesium elements, regardless of the reaction conditions, were lower in the hydrochar than in the process water. On the other hand, it can be observed that for calcium and copper there was an inverse behavior, i.e., a greater incorporation in hydrochar.



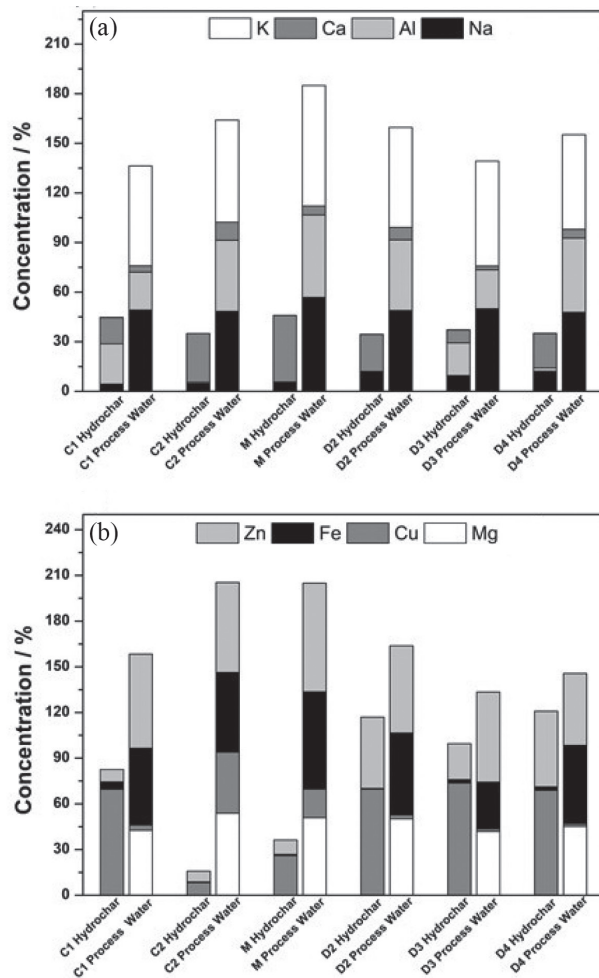


**Figure 5.** Percentage distribution of (a) K, Ca, Al and Na; and (b) Zn, Fe, Cu and Mg remaining in process waters and hydrochars in relation to the total concentration of these nutrients present in the reaction medium by the use of vinasse.

The concentration of Ca in the hydrochars varied as a function of the amount of sulfuric acid added to the reaction medium, since the higher percentages of acid favored the precipitation of higher amounts of calcium as calcium sulfate. The hydrochars D4 and D2, obtained by adding 8.3% acid to the reaction medium, showed higher calcium concentrations (20.9 and 22.4 mg kg<sup>-1</sup>, respectively) than the D3 sample (7.8 mg kg<sup>-1</sup>) produced with 1.7% acid (see Table S1, SI section). The same behavior was observed for hydrochar C2, whose reaction medium was acidified with 8.3% acid, and the Ca concentration was 29.4 mg kg<sup>-1</sup>, while hydrochar C1, produced with 1.7% of acid, presented 15.8 mg kg<sup>-1</sup> of calcium.

The presence of nutrients in the hydrochar reflects directly their ash content. The hydrochars of group C presented ash percentages ranging from 6 to 21%. The high ash content is probably related to the lower precipitation of the organic matter present in the vinasse into hydrochar (see Table 1), thus the inorganic compounds representing

the most part of the recovered mass. For group D the ash percentage varied between 4 and 17%. As the increase in temperature favored the conversion of organic matter into solid carbon, the reactions at 200 °C resulted in a larger mass of carbonaceous material; because of this, the inorganic compounds became responsible for a smaller fraction of the final mass. However, sample D3 showed the highest percentage of ash among the samples of group D produced in the presence of acid. Possibly, that ash value is associated with a higher amount of silicon oxide in this sample, since the content in the hydrochar of the other elements analyzed by FAAS were similar to those found in the other samples of group D.

#### Process water

As shown in Table 2, the lower temperatures (100 and 150 °C) did not favor the conversion of the organic matter present in the vinasse into carbonaceous material and, consequently, there were still high TOC values in the process water of these reactions (groups C and M). On the other hand, the reactions of group D stand out in the reduction of TOC; mainly the reactions D2 and D4, which showed a reduction of approximately 77% of this parameter in relation to vinasse. Additionally, it is worth mentioning that the process waters of the D2 and D4 reactions also showed strong discoloration, with reductions in the actual color of 99.5 and 99.9%, respectively. The discoloration would have its origin, mainly, in the degradation of the organic molecules present in the vinasse.

Further, the data in Table 2 indicate increased process water conductivity with the addition of sulfuric acid. This acid was added to the reaction medium due to its dehydrating properties and the catalytic action of the H<sup>+</sup> ions in the rupture of the complex molecules present in the vinasse. It is important to note that, for group C reactions, the difference in conductivity between the reactions of acid percentage 1.7 and 8.3% (of the order of 70 to 370 mS cm<sup>-1</sup>) was greater than the equivalent reactions of group D (of the order of 70 to 250 mS cm<sup>-1</sup>). In addition, it is observed that for the same group of reactions (C or D), for the acid percentage of 8.3%, reduction of conductivity occurs with an increase in reaction time. These results suggest that the increase in temperature and reaction time led to the reduction of the ion concentration in the reaction medium, either by ion consumption during the carbonization reactions involving the biomass, or because of the precipitation reactions involving cations and anions (see Table S1, SI section, showing the concentration of some ions).



The mass balance was calculated taking into account the amount of each element added (concentration in the vinasse) and retained in both hydrochar and process water. The difference is associated with the amounts leached in the hydrochar washes, which were not quantified by the wash water and therefore were not considered in the mass balance calculations. Therefore, Figure 5 also shows the percentage of the remaining nutrients in the process water. In general, the highest concentration of elements remained in the process water. The reaction C2 exhibited the highest remaining concentration of Cu in the process water (40%), the other samples of process water showed remaining concentrations around 1-18%. The remaining concentration of calcium was only 2-11%, suggesting once again that there was precipitation of this element in the hydrochar, as indicated by the XRD (Figure 3). For Al, the remaining concentrations in the process water varied from 22 to 49%. For reactions with higher acid content (C2, D2 and D4) higher remaining concentrations of Al were found in the process water. The analysis indicated that the elements K, Na, Fe, and Mg are predominantly in the process water and at low relative concentrations in the hydrochar. This would be due to the acid medium favoring neither the precipitation of insoluble phases nor the complexation of these nutrients by the carboxylate groups of the hydrochar.<sup>33</sup>

Thus, the results shown suggest that the reaction medium directly influences the concentration of the nutrients present in hydrochar and in process water. Therefore, these results are very interesting because they suggest that control of the carbonization parameters could influence the final nutrient concentrations in both hydrochar and process water. Taking into account only the concentration of the elements (Table S2, SI section), the increase in temperature and acidity favored a good incorporation of these elements in both hydrochar and process water, while lower acidity and temperature favored high concentration in the process water. Thus, additional treatments of the process water could enable its reuse in the industrial process, its use becoming possible in several stages, since its compositional characteristics are very different from vinasse.

## Conclusions

Among the conditions studied in this work, the reactions with an acid percentage of 8.3% and temperature of 200 °C (D2 and D4) stood out from the others. They produced a larger mass of hydrochar, showing that, among the three factors analyzed, the temperature and percentage of acid has a direct influence on the hydrochar mass recovered. The hydrochars D2 and D4 were more carbonized, although still with low structural

order, presenting a morphology more defined than the others, with spherical particles of sizes in the order of a few micrometers. Additionally, HTC also enabled the incorporation of nutrients into the hydrochars.

Regarding the process water, although reactions D2 and D4 exhibited lower concentrations of TOC, the D4 process water showed greater color reduction. The concentration of nutrients in the process waters deserves special attention in regards to the final destination of the process water, since there were reductions in concentration compared to vinasse; however, some elements are still present in large quantities.

Thus, the hydrothermal treatment of vinasse by HTC proved to be a technically adequate method to treat the vinasse, making it possible to obtain two products: process water and hydrochar, the latter presenting potential for use in agriculture as a soil conditioner, considering its concentration of nutrients. However, some studies are necessary, based on the characteristics of soil, the requirements of the culture, and the concentrations of hydrochar and process water before any application of these two products. Further, maybe a pre-treatment of process water should be required before its application or disposal.

## Supplementary Information

Supplementary information (concentration of nutrients and other elements (Zn, Mg, K, Cu, Fe, Ca, Na, and Al) present in both hydrochar and process water, the instrumental parameters for FAAS analysis and the Pareto chart) is available free of charge at <http://jbcs.sbq.org.br> as PDF file.

## Acknowledgments

The authors thank the Laboratório de Sucoquímica e Química Analítica (UNESP / IBILCE) for providing the FTIR spectrometer. O. P. F. and M. C. B. also acknowledge support from Conselho Nacional de Desenvolvimento Científico e Tecnológico (CNPq; grants 478743 / 2013-0 and 445487 / 2014-3), Fundação Cearense de Apoio ao Desenvolvimento Científico e Tecnológico (FUNCAP; PRONEX PR2-0101-00006.01.00 / 15) and Fundação de Amparo à Pesquisa do Estado de São Paulo (FAPESP; 2014 / 22400-3, 2017 / 26718-6 and 2018 / 15733-7). We also appreciate the scholarship from Coordenação de Aperfeiçoamento de Pessoal de Nível Superior (CAPES). M. C. B. is a recipient of a productivity fellowship by CNPq (307925 / 2012-9). Also, the authors are grateful to Central Analítica-UFC / CT-INFRA / MCTI-SISNANO / Pró-Equipamentos CAPES for providing the SEM.

## References

- Moraes, B. S.; Zaiat, M.; Bonomi, A.; *Renewable Sustainable Energy Rev.* **2015**, *44*, 888.
- Christofoletti, C. A.; Escher, J. P.; Correia, J. E.; Marinho, J. F. U.; Fontanetti, C. S.; *Waste Manage.* **2013**, *33*, 2752.
- Bueno, P. C.; Rubí, J. A. M.; Giménez, R. G.; Ballesta, R. J.; *J. Soils Sediments* **2009**, *9*, 121.
- Marinho, J. F. U.; Correia, J. E.; Marcato, A. C. D. C.; Pedro-Escher, J.; Fontanetti, C. S. *Ecotoxicol. Environ. Saf.* **2014**, *110C*, 239.
- <https://www.embrapa.br/busca-de-noticias/-/noticia/2649716/artigo-surtos-da-mosca-dos-estabulos-proximos-a-usinas-de-cana-de-acucar>, accessed in May 2019.
- Hoarau, J.; Caro, Y.; Grondin, I.; Petit, T.; *J. Water Process Eng.* **2018**, *24*, 11.
- Silva, M. A. S.; Griebeler, N. P.; Borges, L. C.; *Rev. Bras. Eng. Agric. Ambiental* **2007**, *11*, 108.
- Espana-Gamboa, E.; Mijangos-Cortes, J.; Barahona-Perez, L.; Dominguez-Maldonado, J.; Hernandez-Zarate, G.; Alzate-Gaviria, L.; *Waste Manage. Res.* **2011**, *29*, 1235.
- Frohlich, S.; *Br PI 1100736-2 A2*, **2014**.
- Carthery, J. L. A.; Bonkoski, W. A.; Vallero, M. V.; Lima, F. C. B.; Zabeu, C.; Arntsen, B.; *WO 2014/098874 A1* **2014**.
- Coraucci Neto, D.; *Br PI 1106809-4 A2*, **2014**.
- Coraucci Neto, D.; *Br PI 0706144-7 A2*, **2009**.
- Pachere, M. A.; Pistorosi, P. D.; *Br PI 0401563-0 A*, **2005**.
- El-Dib, F. I.; Tawfik, F. M.; Eshaq, G.; Hefni, H. H. H.; ElMetwally, A. E.; *Int. J. Biol. Macromol.* **2016**, *86*, 750.
- Seixas, F. L.; Gimenes, M. L.; Fernandes-Machado, N. R. C.; *Quim. Nova* **2016**, *39*, 172.
- Fagier, M. A.; Ali, E. A.; Tay, K. S.; Abas, M. R. B.; *Int. J. Environ. Sci. Technol.* **2016**, *13*, 1189.
- Barrera, E. L.; Rosa, E.; Spanjers, H.; Romero, O.; Meester, S. D.; Dewulf, J.; *J. Cleaner Prod.* **2016**, *113*, 459.
- Albarez, R.; Chiaranda, B. C.; Ferreira, R. G.; França, A. L. P.; Honório, C. D.; Rodrigues, J. A. D.; Ratusznei, S. M.; Zaiat, M.; *Appl. Biochem. Biotechnol.* **2016**, *178*, 21.
- Poerschmann, J.; Baskyr, I.; Weiner, B.; Koehler, R.; Wedwitschka, H.; Kopinke, F. D.; *Bioresour. Technol.* **2013**, *133*, 581.
- Hu, B.; Wang, K.; Wu, L.; Yu, S. H.; Antonietti, M.; Titirici, M. M.; *Adv. Mater.* **2010**, *22*, 813.
- Titirici, M. M.; White, R. J.; Falco, C.; Sevilla, M.; *Energy Environ. Sci.* **2012**, *5*, 6796.
- Li, L.; Hale, M.; Olsen, P.; Berge, N. D.; *Waste Manage.* **2014**, *34*, 2185.
- Kambo, H. S.; Dutta, A.; *Renewable Sustainable Energy Rev.* **2015**, *45*, 359.
- Reza, M. T.; Andert, J.; Wirth, B.; Busch, D.; Pielert, J.; Lynam, J. G.; *Appl. Bioenergy* **2014**, *1*, 11.
- Yoshimura, M.; Byrappa, K.; *J. Mater. Sci.* **2008**, *43*, 2085.
- Libra, J. A.; Ro, K. S.; Kammann, C.; Funke, A.; Berge, N. D.; Neubauer, Y.; Titirici, M. M.; Fühner, C.; Bens, O.; Kern, J.; Emmerich, K. H.; *Biofuels* **2011**, *2*, 71.
- Poerschmann, J.; Weiner, B.; Wedwitschka, H.; Baskyr, I.; Koehler, R.; Kopinke, F.-D.; *Bioresour. Technol.* **2014**, *164*, 162.
- Tekin, K.; Karagöz, S.; Bektaş, S.; *Renewable Sustainable Energy Rev.* **2014**, *40*, 673.
- Medick, J.; Teichmann, I.; Kemfert, C.; *Energy Policy* **2018**, *123*, 503.
- Stemann, J.; Erlach, B.; Ziegler, F.; *Waste Biomass Valorization* **2013**, *4*, 441.
- Lucian, M.; Fiori, L.; *Energies* **2017**, *10*, 211.
- Melo, C. A.; Soares Jr., F. H.; Bisinoti, M. C.; Moreira, A. B.; Ferreira, O. P.; *Waste Biomass Valorization* **2017**, *8*, 1139.
- Silva, C. C.; Melo, C. A.; Soares Jr., F. H.; Moreira, A. B.; Ferreira, O. P.; Bisinoti, M. C.; *Bioresour. Technol.* **2017**, *237*, 213.
- Oliveira, I.; Blöhse, D.; Ramke, H. G.; *Bioresour. Technol.* **2013**, *142*, 138.
- Funke, A.; Ziegler, F.; *Biofuels, Bioprod. Biorefin.* **2010**, *4*, 160.
- Du, Z.; Hu, B.; Shi, A.; Ma, X.; Cheng, Y.; Chen, P.; Liu, Y.; Lin, X.; Ruan, R.; *Bioresour. Technol.* **2012**, *126*, 354.
- Rillig, M. C.; Wagner, M.; Salem, M.; Antunes, P. M.; George, C.; Ramke, H. G.; Titirici, M. M.; Antonietti, M.; *Appl. Soil Ecol.* **2010**, *45*, 238.
- Fregolente, L. G.; Moreira, A. B.; Ferreira, O. P.; Bisinoti, M. C.; *Br PI 102015003018-5*, **2015**.
- American Public Health Association (APHA), American Water Works Association, Water Environment Federation; *Standard Methods for the Examination of Water and Wastewater*, 21<sup>st</sup> ed.; APHA: Washington, D. C., 2005.
- United States Environmental Protection Agency (US EPA); *Method 3050B: Acid Digestion of Sediments, Sludges, and Soils*; US EPA: Washington, D. C., 1996.
- United States Environmental Protection Agency (US EPA); *Method 3010A: Acid Digestion of Aqueous Samples and Extracts for Total Metals for Analysis by FLAA or ICP Spectroscopy*; US EPA: Washington, D. C., 1992.
- Kang, S.; Li, X.; Fan, J.; Chang, J.; *Ind. Eng. Chem. Res.* **2012**, *51*, 9023.
- Parshetti, G. K.; Kent Hoekman, S.; Balasubramanian, R.; *Bioresour. Technol.* **2013**, *135*, 683.
- Sevilla, M.; Fuertes, A. B.; *Carbon* **2009**, *47*, 2281.
- Sevilla, M.; Maciá-Agulló, J. A.; Fuertes, A. B.; *Biomass Bioenergy* **2011**, *35*, 3152.
- Sevilla, M.; Fuertes, A. B.; *Chem. - Eur. J.* **2009**, *15*, 4195.
- Spokas, K. A.; *Carbon Manage.* **2010**, *1*, 289.
- Srinivasan, P.; Sarmah, A. K.; Smernik, R.; Das, O.; Farid, M.; Gao, W.; *Sci. Total Environ.* **2015**, *512-513*, 495.

49. Sun, X.; Li, Y.; *Angew. Chem., Int. Ed.* **2004**, *43*, 597.
50. Liu, Z.; Zhang, F. S.; Wu, J.; *Fuel* **2010**, *89*, 510.
51. Özçimen, D.; Ersoy-Meriçboyu, A.; *Renewable Energy* **2010**, *35*, 1319.
52. Makreski, P.; Jovanovski, G.; Dimitrovska, S.; *Vib. Spectrosc.* **2005**, *39*, 229.
53. Handke, M.; Mozgawa, W.; *Vib. Spectrosc.* **1993**, *5*, 75.
54. Unur, E.; *Microporous Mesoporous Mater.* **2013**, *168*, 92.
55. White, R. J.; Antonietti, M.; Titirici, M.-M.; *J. Mater. Chem.* **2009**, *19*, 8645.
56. Wang, Y.; Yang, R.; Li, M.; Zhao, Z.; *Ind. Crops Prod.* **2015**, *65*, 216.
57. Romero-Anaya, A. J.; Ouzzine, M.; Lillo-Ródenas, M. A.; Linares-Solano, A.; *Carbon* **2014**, *68*, 296.

Submitted: February 12, 2019

Published online: June 3, 2019

